

Characterizing Oligosaccharides Using Injected-Ion Mobility/Mass Spectrometry

Yansheng Liu and David E. Clemmer*

Department of Chemistry, Indiana University Bloomington, Indiana 47405

Injected-ion mobility/mass spectrometry techniques have been used to measure the reduced ion mobilities for negatively charged raffinose, melezitose and α -, β -, and γ -cyclodextrins formed by electrospray ionization. At low injection energies, the mass spectra are dominated by negatively charged (deprotonated) parent ions. At high injection energies, the mass spectra recorded for the cyclodextrins and raffinose display peaks that result from cross-ring cleavage of individual sugar units. Melezitose dissociates by cleavage of the glycosidic bonds. The ion mobility distributions can be used to distinguish between different isomeric forms of parent and fragment ions having the same mass-to-charge ratios.

The sequences and three-dimensional structures of carbohydrates play a large role in many biological recognition processes. Analysis of these species is an arduous problem because of the large number of different sugar units and multitude of possible branching patterns and conformations that can exist.¹ Nuclear magnetic resonance has been used to provide detailed structural information for carbohydrates and glycoconjugates but is often constrained by the demands of large sample quantities.² Mass spectrometry (MS)-based methods that utilize new ionization sources such as fast atom bombardment (FAB),³ matrix-assisted laser desorption/ionization (MALDI),⁴ and electrospray ionization (ESI)⁵ have emerged for characterization of sequences of some biomolecules. For many biomolecules with linear covalent sequences, such as oligonucleotides and oligopeptides, MS-based strategies⁶ can unambiguously characterize the biopolymer sequence. The complex structures of carbohydrates present a unique challenge for MS methods because different structural isomers have identical mass-to-charge (m/z) ratios.

In this paper, we report the first application of ion mobility methods for the analysis of oligosaccharides. Ion mobility techniques separate ions based on differences in their mobilities through a buffer gas.^{7–13} Compact isomers have higher mobilities than diffuse ones, making it possible to distinguish between

different isomers. Here, we show that this method can be used to induce fragmentation in oligosaccharides and distinguish between different isomers or conformations having the same m/z ratios. We have examined the fragmentation patterns and mobilities of five simple oligosaccharides: raffinose and melezitose, which are each comprised of three sugar units; and α -, β -, and γ -cyclodextrins (CD), which have cyclic structures and contain six, seven, and eight sugar units, respectively. These have been produced by ESI as negatively charged deprotonated ions.

A number of studies have used MS methods to characterize oligosaccharides. FAB,¹⁴ laser desorption/ionization,^{15–17} and in-source pyrolysis chemical ionization techniques¹⁸ have been used to analyze molecular weights of parent and fragment ions. Recently, ESI¹⁹ and MALDI^{20,21} have been used to examine carbohydrates having larger molecular weights. Differences in the fragmentation patterns observed for oligosaccharides have been investigated as a means of distinguishing between isobaric ions by MS.^{17,22}

EXPERIMENTAL SECTION

The experimental apparatus was constructed in-house, and a schematic diagram is shown in Figure 1. The sugars used in this study, raffinose (>99%) melezitose, α -CD (99%), β -CD, and γ -CD were obtained from Sigma and used without further purification. Negatively charged (deprotonated) oligosaccharide ions were formed at atmospheric pressure by electrospraying a solution containing $\sim 10^{-4}$ M of the oligosaccharide in a 49:49:2 water/ acetonitrile/ammonium hydroxide solution. Electrosprayed droplets enter a variable-temperature, differentially pumped desolvation

- (1) Kennedy, J. F.; White, C. A. *Bioactive Carbohydrates in Chemistry, Biochemistry and Biology*, 1st ed.; Ellis Horwood Limited: Chichester, West Sussex, England, 1983.
- (2) Vliegenthart, J. F. G.; Dorland, L.; Van Halbeek, H. *Adv. Carbohydr. Chem. Biochem.* **1983**, *41*, 209–374.
- (3) Barber, M.; Bordoli, R. D.; Sedwick, R. D.; Tyler, A. N. *J. Chem. Soc., Chem. Commun.* **1981**, 325–327.
- (4) Karas, M.; Hillenkamp, F. *Anal. Chem.* **1988**, *60*, 2299–2301.
- (5) Fenn, J. B.; Mann, M.; Meng, C. K.; Wong, S. F.; Whitehouse, C. M. *Science* **1989**, *246*, 64–71.
- (6) See, for example: Biemann, K. *Annu. Rev. Biochem.* **1992**, *61*, 977–1010. Ni, J.; Pomerantz, S. C.; Rozenski, J.; Zhang, Y.; McCloskey, J. A. *Anal. Chem.* **1996**, *68*, 1989–1999, and references therein.
- (7) Hagen, D. F. *Anal. Chem.* **1979**, *51*, 870–874.
- (8) Tou, J. C.; Boggs, G. U. *Anal. Chem.* **1976**, *48*, 1351–1357.

- (9) Carr, T. W. *J. Chromatogr. Sci.* **1977**, *15*, 85–88.
- (10) Karpas, Z.; Cohen, M. J.; Stimac, R. M.; Wernlund, R. F. *Int. J. Mass Spectrom. Ion Processes* **1986**, *83*, 163–175.
- (11) St. Louis, R. H.; Hill, H. H. *Crit. Rev. Anal. Chem.* **1990**, *21*, 321–355.
- (12) von Helden, G.; Hsu, M. T.; Kemper, P. R.; Bowers, M. T. *J. Chem. Phys.* **1991**, *95*, 3835–3837.
- (13) Jarrold, M. F. *J. Phys. Chem.* **1995**, *99*, 11–21.
- (14) See, for example: Peter-Katalinic, J. *Mass Spectrom. Rev.* **1994**, *13*, 77–98, and references therein.
- (15) Coates, M. L.; Wilkins, C. L. *Anal. Chem.* **1987**, *59*, 197–200.
- (16) Lam, Z.; Comisarow, M. B.; Dutton, G. G. S. *Anal. Chem.* **1988**, *60*, 2304–2306.
- (17) Spengler, B.; Dolce, J. W.; Cotter, R. J. *Anal. Chem.* **1990**, *62*, 1731–1737.
- (18) Lomax, J. A.; Boon, J. J.; Hoffmann, A. *Carbohydr. Res.* **1991**, *221*, 219–233.
- (19) For a recent review, see: Reinhold, V. N.; Reinhold, B. B.; Chan, S. *Methods Enzymol.* **1996**, *271*, 377–402.
- (20) Penn, S. G.; Cancilla, M. T.; Lebrilla, C. B. *Anal. Chem.* **1996**, *68*, 2331–2339.
- (21) For a recent review, see: Harvey, D. J. *J. Chromatogr., A* **1996**, *720*, 429–446.
- (22) See, for example: Mulrone, B.; Traeger, J. C.; Stone, B. A. *J. Mass Spectrom.* **1995**, *30*, 1277–1283. Dongre, A. R.; Wysocki, V. H. *Org. Mass Spectrom.* **1994**, *29*, 700–702. Fura, A.; Leary, J. A. *Anal. Chem.* **1993**, *65*, 2805–2811, and references therein.

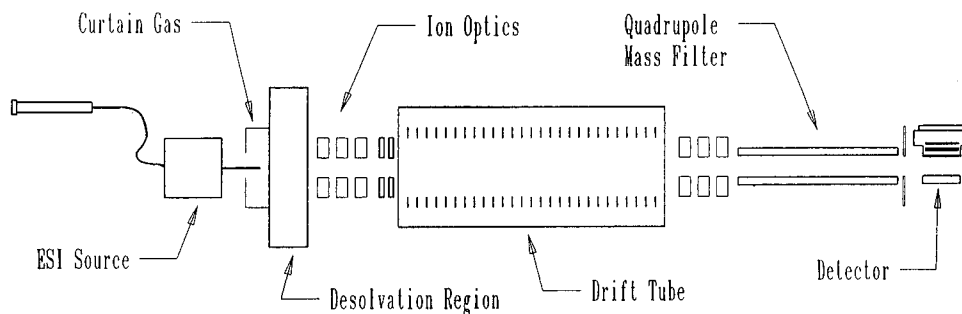


Figure 1. Schematic diagram of the experimental apparatus.

region (~ 1 – 10 Torr) through a 0.025 cm diameter aperture. Ions exit this region through another 0.025 cm diameter aperture where they enter a high-vacuum region (10^{-4} – 10^{-5} Torr), are focused into a low-energy ion beam, and are injected into the drift tube. The injection energy is defined by the voltage difference (multiplied by the charge state of the ion) between the exit of the high-pressure ion source and the drift tube entrance. As shown below, the injection energy can be varied in order to induce fragmentation.

The drift tube is 32.4 cm long and contains ~ 3 Torr of 300 K nitrogen buffer gas. Nitrogen was chosen as the buffer gas, instead of He, which has been used recently in ion mobility studies,^{12,13} because it provides a greater center-of-mass collision energy for the initial collisions as ions enter the drift tube. The entrance and exit apertures of the drift tube are 0.08 cm in diameter, and 27 equally spaced electrostatic lenses ensure a uniform electric field along the axis of the ion beam. The drift tube body is made of stainless steel with Teflon spacers at each end, which electrically isolate the entrance and exit plates. Except where noted, data were recorded using a drift field of 49.4 V cm^{-1} . After exiting the drift tube, ions are focused into a quadrupole mass spectrometer (Extrel) that can be set to transmit a specific mass (for measurements of ion mobility distributions) or scanned in order to monitor fragmentation patterns. Ions are detected using an off-axis collision dynode/dual microchannel plate detection system that was also constructed in-house.

Ion mobility distributions were recorded by injecting 10 – 30 μs pulses of ions into the drift tube and recorded the arrival time distribution at the detector using a multichannel scaler. Different isomers or conformations of the ions that are formed during electrospray or upon injection into the drift tube can be separated because of differences in their mobilities through the buffer gas.²³ Ions with small collision cross sections with the buffer gas will have higher mobilities than those with larger cross sections. As in electrophoresis, the mobility also depends on the charge state, as shown recently for multiply charged protein ions formed by ESI.^{24,25}

The arrival time is a composite of the time the ions spend in the drift tube and the time required for the ion pulse to travel through other portions of the instrument before reaching the detector. Thus, it is necessary to subtract the flight time of the ions when no buffer gas is present and also account for differences

in the ions' kinetic energies at the exit of the drift tube, with and without buffer gas. In these studies, the differences between the arrival times and drift times were between 180 and 270 μs .

A series of diagnostic studies of the drift velocity as a function of the applied drift voltage show that all the ions studied here drift through the buffer gas in the low-field limit.²⁶ Under these conditions, the drift velocity depends linearly upon the drift voltage. The experimentally derived reduced mobility is determined from²⁶

$$K_o = \frac{L}{t_D} \frac{P}{E} \frac{273.2}{760 T} \quad (1)$$

where t_D is the average drift time, E is the electric field, L is the length of the drift tube, and P is the buffer gas pressure in Torr. All of the parameters E , L , P , and t_D can be precisely measured such that the reproducibility of these experiments is excellent. Any two measurements of the mobility almost always agree to within 1% (percent relative uncertainty). The uncertainty associated with the accuracy of these measurements may be slightly greater due to systematic effects such as penetration of the ions into the drift tube upon injection (which decreases the effective length of the drift tube). Ion mobility distributions recorded at varying injection energies and buffer gas pressures yield similar mobilities suggesting that these effects are small; we estimate that our mobilities are accurate to within a few percent.

Although the reproducibility of the mobility measurement is excellent, the ability to resolve two isomers or conformations that have similar mobilities is more limited. In the distributions that are shown, the experimental resolving power ($t_D/\delta t$, where δt is the full width at half-maximum of the mobility peak) is 50 . Therefore, in order to distinguish an equal fraction of two isomers or conformers in a mixture, they must have mobilities that differ by more than $\sim 2\%$.

As ions are injected into the drift tube, they are rapidly heated as their kinetic energies are thermalized by collisions with the buffer gas. Further collisions cool the ions to the temperature of the buffer gas. This heating/cooling cycle occurs at the entrance of the drift tube such that it is possible to generate and record mobility distributions for fragment ions. As noted above, mobilities recorded at different injection energies are very similar, indicating that ions do not penetrate significantly into the drift tube during the injection process. Ideally, it is desirable to mass select ions before injection into the drift tube; however, as shown in Figure 1, our current instrument is not configured for this. For

(23) Clemmer, D. E.; Hudgins, R. R.; Jarrold, M. F. *J. Am. Chem. Soc.* **1995**, *117*, 10141.

(24) Wittmer, D.; Chen, Y. H.; Luckenbill, B. K.; Hill, H. H., Jr. *Anal. Chem.* **1994**, *66*, 2348–2355.

(25) Shelimov, K. B.; Clemmer, D. E.; Hudgins, R. R.; Jarrold, M. F. *J. Am. Chem. Soc.* **1997**, *119*, 2240–2248.

(26) Mason, E. A.; McDaniel, E. W. *Transport Properties of Ions in Gases*; Wiley: New York, 1988.

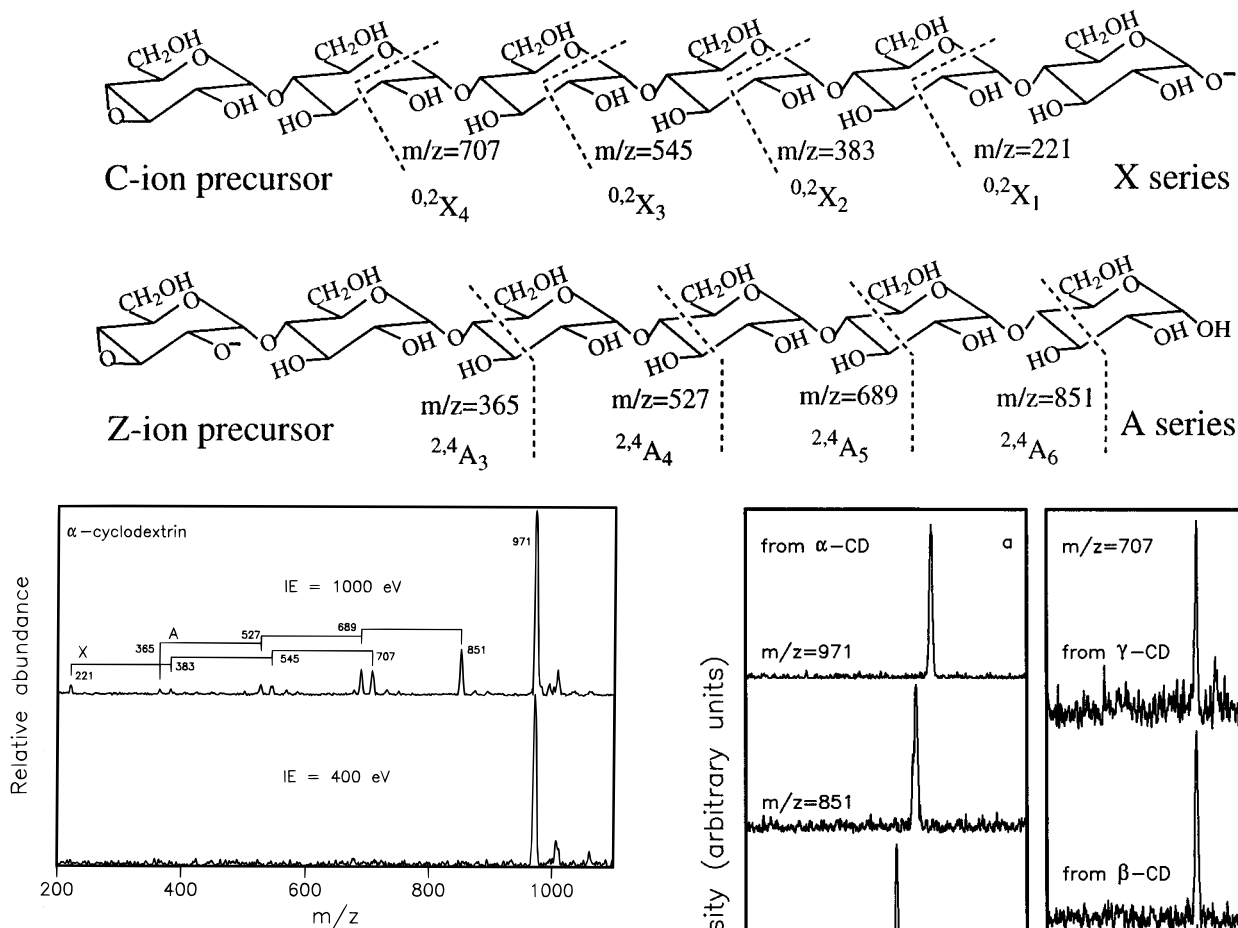


Figure 2. Mass spectra recorded for α -cyclodextrin when ions are injected into a drift tube using injection energies of 400 (bottom) and 1000 eV (top). The fragments that are observed at high injection energies can be assigned to the known X and A series fragmentation patterns, as shown.

the present studies, mass spectra at low injection energies and other studies where the buffer gas was removed are dominated by deprotonated parent ions; from this, it is clear that the fragment ions are formed during the injection process.

RESULTS AND DISCUSSION

Fragmentation of Cyclodextrins. Figure 2 shows the ESI mass spectra obtained for α -CD when ions are injected into the drift tube using injection energies of 400 or 1000 eV. At 400 eV, the mass spectrum is dominated by a peak at $m/z = 971$, which corresponds to the deprotonated parent ion.²⁷ As the injection energy is increased to ~ 700 eV (not shown), a series of lower m/z peaks corresponding to fragment ions is observed. The relative intensities of the fragment ions increase as the injection energy is increased to 1000 eV. Similar behavior is observed in the β - and γ -CD systems. The peaks observed in the cyclodextrin mass spectra can be explained by cross-ring cleavages which produce A and X series fragments.²⁸ Individual fragments within a series differ by 162 amu, the formula weight of the amylose

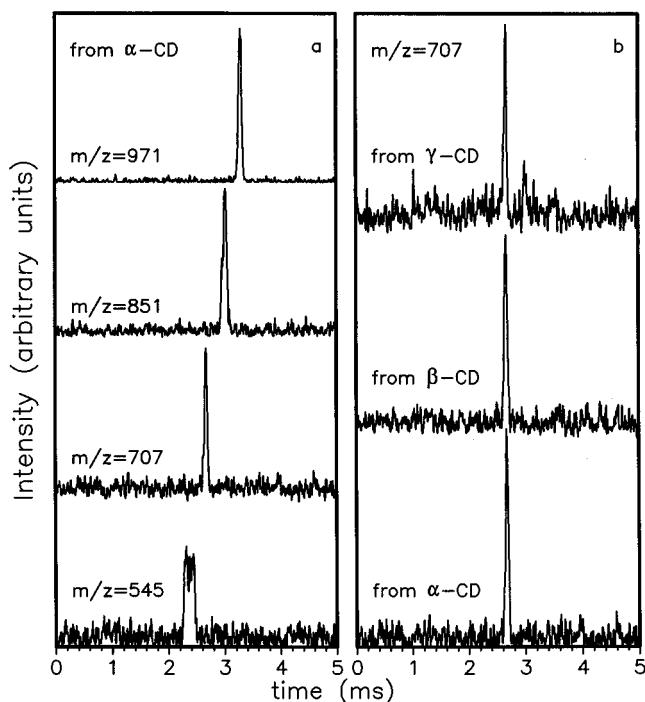


Figure 3. Ion mobility distributions recorded at an injection voltage of 1000 eV for α -cyclodextrin and several fragments (a) in nitrogen buffer gas. The data have been normalized to a buffer gas pressure of 2.9 Torr. (b) Ion mobility distributions that have been recorded for the $m/z = 707$ fragment that was formed by collision-induced dissociation of α -, β -, and γ -cyclodextrins. These data have also been normalized to a buffer gas pressure of 2.9 Torr.

unit. The origin of this fragments is illustrated in Chart 1 and discussed in more detail below.

Ion Mobility Distributions for Cyclodextrins and Fragments. Figure 3 shows ion mobility distributions recorded for deprotonated α -CD ($m/z = 971$) and several example fragment peaks at $m/z = 545$, 707, and 851, respectively. The $m/z = 707$ and 851 distributions are each dominated by a single narrow peak, suggesting that each ion corresponds to a single isomer. The $m/z = 545$ fragment shows multiple features in the ion mobility distribution; here multiple forms having identical m/z values but different three-dimensional structures must exist. Smaller fragments have shorter drift times because of their smaller collision cross sections with the buffer gas.

(27) Under some conditions, we observe a peak that corresponds to deprotonated dimer ions. This peak is significantly smaller (at least a factor of 3) than the parent monomer ion.

(28) This assignment uses the systematic nomenclature described by: Domon, B.; Costello, C. E. *Glycoconjugate J.* **1988**, *5*, 397–409.

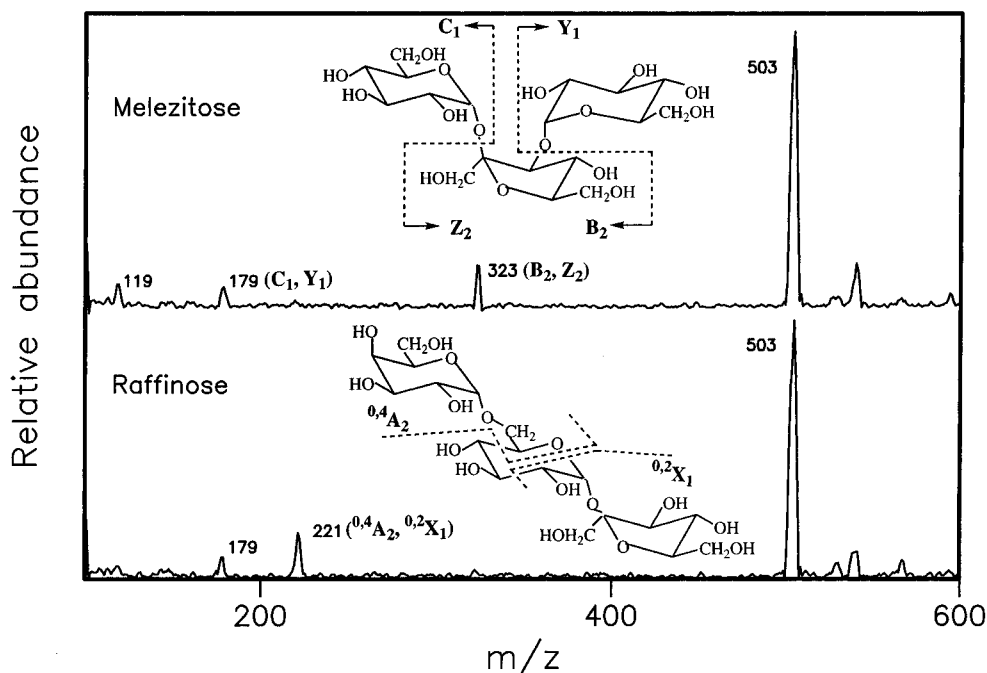


Figure 4. Mass spectra showing fragmentation of melezitose and raffinose, recorded using an injection energy of 1000 eV. These spectra are dominated by the deprotonated parent at $m/z = 503$. Schematic representations of the different isomeric structures of these ions are also shown. The dashed lines indicate the bond cleavages necessary to form the $m/z = 221$ and $m/z = 323$ fragments observed for raffinose and melezitose, respectively.

The virtually identical fragmentation patterns observed for all three cyclodextrins make it possible to examine a single fragment that originates from each of the three precursor ions. Figure 3 also shows ion mobility distributions recorded for the $m/z = 707$ fragment ion that is formed during CID of each of the three sugars. Each spectrum is dominated by a single narrow peak at 2.662, 2.675, and 2.673 ms for fragments formed from CID of the α -, β -, and γ -CD ions, respectively. The range of values varies by only 0.5% and is typical of the relative uncertainties of different measurements in these studies. The indistinguishable drift times indicate that the $m/z = 707$ fragments have the same collision cross sections. This suggests that these ions have the same isomeric structure, as would be expected from dissociation of these three precursors. In addition, there are no observable differences due to formation of different gas-phase conformations during the fragmentation process. Thus, either these fragment ions have similar conformations (possibly even identical) or different conformations have collision cross sections that are indistinguishable within our 0.5% experimental uncertainty. The other common fragments observed for α -, β -, and γ -CD display similar behavior. This includes the multiple features observed for the $m/z = 545$ peak that was studied for α - and β -CD, although the relative abundances of the different features vary slightly for different precursors.

Distinguishing between Different Sugar Isomers Having Identical m/z Ratios. In order to examine the ability of ion mobility methods to distinguish between different sugar isomers having the same m/z ratios, we have examined the two residue sugars melezitose [α -D-Glcp-(1 \rightarrow 3)- β -D-Fruf-(2 \leftrightarrow 1)- α -D-Glcp] and raffinose [α -D-Galp-(1 \rightarrow 6)- α -D-Glcp-(1 \leftrightarrow 2)- β -D-Fruf] which differ in sequence, linkage, and anomeric configuration. Both have a molecular weight of 504 amu and form the deprotonated parent ion ($m/z = 503$) upon negative ion ESI. Figure 4 shows the fragmentation mass spectra for melezitose and raffinose that are

obtained by injecting ions into the drift tube at 1000 eV. Under these conditions, melezitose displays a fragment at $m/z = 323$ that can be explained by cleavage of one of the two possible glycosidic bonds, as shown. Raffinose dissociates to form the $m/z = 221$ fragment ion, a result that can be explained by cross-ring cleavage involving either the 2-0 or 4-0 bonds of the center residue (also shown in Figure 4).

The ion mobility distributions for ions having m/z ratios that are identical (i.e., $m/z = 503$ from melezitose and raffinose, and the $m/z = 221$ fragment ions from raffinose and α -CD) are shown in Figure 5. The $m/z = 503$ parent ions for melezitose and raffinose display narrow peaks, with drift times of 2.135 and 2.162 ms, respectively: a 1.3% difference, which is slightly larger than our experimental uncertainties. From this we conclude that the ions have different structures. A larger difference in drift times is observed for the $m/z = 221$ fragments formed from CID of α -CD and raffinose, having drift times of 1.419 and 1.493 ms, respectively. This 5.2% difference is easily distinguished. The ion mobility distribution for the $m/z = 323$ fragment formed from CID of melezitose displays two distinct peaks, showing that distinct conformers or isomers are present. The schematic diagram for melezitose in Figure 4 delineates two possible dissociation pathways leading to different isomers of the $m/z = 323$ ion. It seems likely that the different features for the $m/z = 323$ ion mobility distribution correspond to distinct fragmentation pathways. An interesting feature of the $m/z = 323$ fragments that are observed for melezitose is the large difference in the mobilities of these isomers. The isomer arriving near 2.1 ms has a mobility that is near the mobility measured for the deprotonated melezitose parent ion. Formation of this isomer is the favored fragmentation pathway at this injection energy.

Figure 6 shows a plot of the inverse reduced ion mobilities for all of the deprotonated parent and fragment ions that were studied here. To a first approximation, the increase in inverse

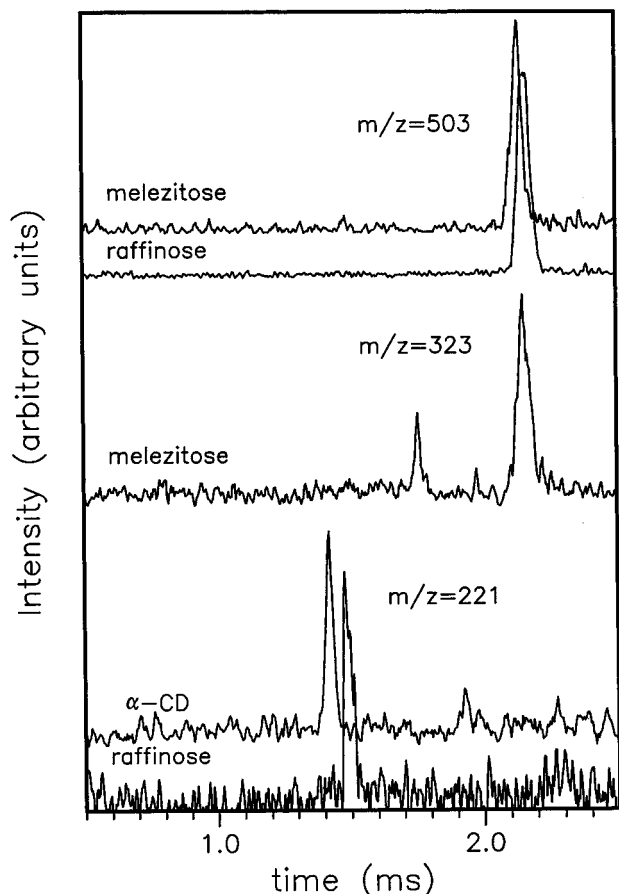


Figure 5. Ion mobility distributions recorded for $m/z = 503$ parent ions of raffinose and melezitose. Also shown are the ion mobility distributions recorded for the $m/z = 221$ fragment observed upon collision-induced dissociation of α -cyclodextrin and raffinose and the $m/z = 323$ fragment of melezitose. These data have been normalized to a buffer gas pressure of 2.9 Torr.

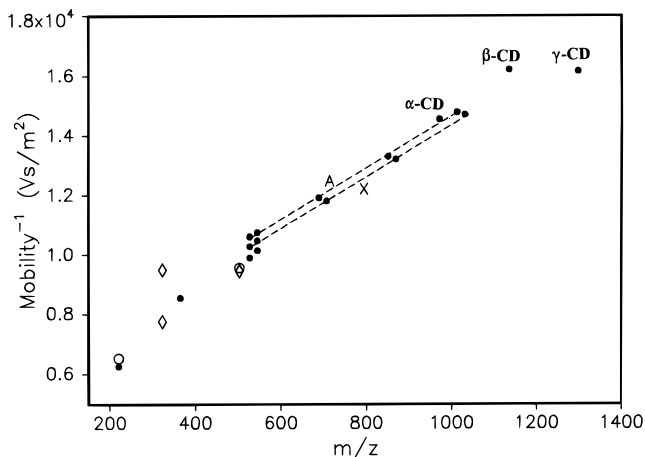


Figure 6. Inverse reduced mobilities derived using eq 1 from ion mobility distributions for oligosaccharide and fragment ions in nitrogen buffer gas. Solid circles show the values obtained for α -, β -, and γ -cyclodextrins and related fragments. The open diamonds show data obtained for melezitose, and the open circles correspond to mobilities derived for raffinose. The dashed lines show that the X and A series fragments appear to have related mobilities.

mobility as a function of increasing m/z is fairly systematic, a result that comes about from the increase in physical size of the ions. However, the variations that are observed provide important clues about the structures of different ions. The inverse mobilities of

the deprotonated α -, β -, and γ -CD parents do not increase systematically. The inverse mobility of β -CD is a factor of ~ 1.1 greater than α -CD; however, γ -CD has a slightly smaller inverse mobility than β -CD. The increase in inverse mobility for β -CD compared with α -CD is similar to the changes observed within both the X and A series fragment ions differing by single residues and suggests that addition of each residue results in a systematic increase in the average collision cross section of the ion. The smaller inverse mobility for γ -CD suggests that this ion has a different three-dimensional structure. This eight-residue sugar is the largest studied here and may be capable of sampling smaller configurations because of increased noncovalent interactions between sugar units that stabilize more folded forms.

Another interesting feature of these data is that the X and A series fragments appear to fall into two families of isomers that can be identified based not only on their masses but also on their mobilities. The X series fragments have molecular weights that are 18 amu above the A series fragments but have inverse mobilities that are consistently $\sim 0.8\%$ smaller. We are currently testing methods for comparing these experimental mobilities (measured in N_2) to those calculated for different trial isomer structures in order to gain a more detailed understanding of the structures of these ions. Analogous methods have proven to be extremely powerful for deducing structures of gas-phase ions from mobilities recorded in He.^{12,13} This should allow us to address subtle differences in the structures of these ions (e.g., rearrangements associated with ring opening).

Finally, the low m/z ions (below 600) exhibit large differences in inverse mobilities. This is particularly noteworthy for the $m/z = 323$ fragment observed upon CID of melezitose. Here, as noted above, one species has an inverse mobility that is similar to that observed for the parent ($m/z = 503$) ion. This suggests that the $m/z = 323$ fragment ion has a much more open structure than the parent. Large differences in the mobilities of ions in this size range have been observed previously for systems involving carbon clusters.^{12,29} These have been attributed to large structural differences that arise from strong directional bonds of carbon which result in vastly different cluster isomer structures (e.g., carbon rings and fullerenes), depending on the hybridization states of the carbon atoms. Sugars also contain many strong directional covalent bonds and differences in their bonding patterns may lead to large differences in mobilities.

Origin of CID Fragments. The origin of these X and Z series fragments can be understood by considering Chart 1. Previous work has suggested that deprotonation of sugars to form a negatively charged ion may result in spontaneous cleavage of the glycosidic bond.^{28,30} In the cyclic oligosaccharides studied here, glycosidic bond cleavage will form a linear chain of sugar residues and the precise structure of the end residues will depend on the location of the charge and the exact rearrangement of protons that occurs during bond cleavage. Chart 1 shows two reasonable structures, which following existing nomenclature,²¹ correspond to the C and Z ions.³¹ By cleaving the C-ion precursor across the 2–0 bonds of the sugar, the X series fragments having $m/z =$

(29) Clemmer, D. E.; Jarrold, M. F. *J. Am. Chem. Soc.* **1995**, *117*, 8841.

(30) Barber, M.; Bordoli, R. S.; Sedgwick, R. D.; Vickerman, J. C. *J. Chem. Soc., Faraday Trans. 1* **1982**, *78*, 1291–1296.

(31) The designation of precursor ions as C and Z in the cyclodextrin system is somewhat arbitrary because of the symmetric nature of the cyclodextrin system. These ions could also be designated as B and Y ions.

707, 545, 383, and 221 are formed. Fragmentation of the Z-ion precursor across the 2-4 bonds of the sugar ring forms the A series fragments having $m/z = 851, 689, 527, \text{ and } 365$. The mass spectra also show smaller peaks that correspond to other known fragmentation patterns, but ion signals for these features were too small to measure mobilities.

The cross-ring bond cleavage patterns described above for cyclodextrins are somewhat different from the other previously observed oligosaccharide fragmentation patterns, which appear to predominantly dissociate by cleavage of glycosidic bonds.^{17,32-34} Differences in fragmentation patterns between protonated and deprotonated states have been noted previously,³⁴ and other differences that appear to arise from variations in target gas composition and collision energy have also been reported.^{35,36} Cross-ring fragmentation patterns such as those observed here offer advantages for sequencing, because the locations of branched sites can be identified from the mass shifts.

-
- (32) Ngoka, L. C.; Gal, J.-F.; Lebrilla, C. B. *Anal. Chem.* **1994**, *66*, 692-698.
(33) Yamagaki, T.; Ishizuka, Y.; Kawabata, S.; Nakanishi, H. *Rapid Commun. Mass Spectrom.* **1996**, *10*, 1887-1890.
(34) Carroll, J. A.; Ngoka, L.; Beggs, C. G.; Lebrilla, C. B. *Anal. Chem.* **1993**, *65*, 1582-1587.
(35) Lemoine, J.; Fournet, B.; Despeyroux, D.; Jennings, K. R.; Rosenberg, R.; de Hoffmann, E. *J. Am. Soc. Mass Spectrom.* **1993**, *4*, 197-203.
(36) Lipniunas, P. H.; Townsend, R. R.; Burlingam, A. L.; Hindsgaul, O. *J. Am. Soc. Mass Spectrom.* **1996**, *7*, 182-188.

CONCLUSIONS

We have shown that ion mobility/MS methods can be used to distinguish between oligosaccharide isomers having identical m/z ratios. By operating the ion mobility instrument in the injected-ion mode, it is possible to induce fragmentation as ions enter the drift tube and record mobilities for parent and fragment ions. The fragment peaks that are observed can be understood by cross-ring cleavages which form the X and A series fragment ions. The ability to induce fragmentation and measure mobilities for these species provides additional structural information that complements MS- and MS/MS-based sequencing approaches. Further work that addresses the assignment of different conformations based on comparison of the experimental mobilities to those calculated for trial ion structures is currently underway in our laboratory, and these comparisons should allow us to be making unambiguous assignments of the different isomers.

ACKNOWLEDGMENT

We are grateful for many stimulating discussions with Dr. Yehia Mechref and Professor Milos Novotny. This work was supported by National Science Foundation (Grant CHE-9625199).

Received for review February 5, 1997. Accepted April 24, 1997.[⊗]

AC9701344

[⊗] Abstract published in *Advance ACS Abstracts*, June 1, 1997.